Supporting Information

A Cuprous [4×4] Grid: Single-Crystal to Single-Crystal Transformation and Fading of Luminescence by Solvent Inclusion

Fei Yu,[†] Jia-Qian Li,[†] Mohamedally Kurmoo,[§] Jing-Lin Zuo*,[†]

[†] *State Key Laboratory of Coordination Chemistry, School of Chemistry and Chemical Engineering, Collaborative Innovation Center of Advanced Microstructures, Nanjing University, Nanjing, 210023, China.*

[§] *Institut de Chimie de Strasbourg, CNRS UMR7177, Université de Strasbourg, 4 rue Blaise Pascal, Strasbourg 67070, France.*

Materials. All chemicals and solvents were obtained from commercial sources and utilized without further purification.

Synthesis of ligand. The ligand H_2L was prepared according to a previous report.[S1]

Measurements. The C, H and N microanalyses were carried out with a Vario Micro Cube elemental analyzer. Powder X-ray diffraction (PXRD) patterns were recorded at 293 K on a D8 ADVANCE (Cu *Kα1*, λ = 1.54056 Å; *Kα2*, λ = 1.54439 Å) powered at 40 kV and 40 mA. The powder samples were prepared by crushing the crystals and the PXRD scanned from 5 to 50° at a rate of 5°/min. Calculated PXRD patterns were generated using Mercury 3.9 (Fig. S1).[S2] Thermogravimetric analyses (TGA) were performed on a NETZSCH STA 449 *F*3 Jupiter TGA instrument in flowing N_2 at a heating rate of 5 °C per minute in the range of 40 to 1200 °C (Fig. S2). Samples for infrared (IR) spectroscopy were prepared as KBr pellets, and spectra were recorded in the 400–4000 cm range using a Vector22 Bruker spectrophotometer. Electron paramagnetic resonance (EPR) spectra were recorded on a Bruker ER-420 spectrometer with a 100 kHz magnetic field in the X band at room temperature (RT). X-ray photoelectron spectroscopy (XPS) studies were performed using a ThermoFisher ESCALAB250 X-ray photoelectron spectrometer (powered at 150 W) using Al K radiation (λ = 8.357 Å). Magnetization measurements for polycrystalline samples were performed on a Quantum Design MPMS-SQUID-VSM magnetometer in the temperature range from 1.8 to 300 K for direct current (dc) applied fields ranging from 0 to 7 T. **X-ray Structure Determination.** The single-crystal X-ray diffraction data for **Cu_{16}**, **Cu_{16}·$4H_2O$** and

Cu_{16}·$2CH_3OH$ were collected on a Bruker D8 VENTURE diffractometer with a PHOTON 100 CMOS detector equipped with a Mo-target X-ray tube (λ = 0.71073 Å) at T = 150 K by using the φ-ω scan technique. Data of **Cu_{16}·$2C_2H_5OH$** were collected on MarCCD MX300 in BL17B beamline of National Facility for Protein Science Shanghai (NFPS) at Shanghai Synchrotron Radiation Facility (SSRF) at 100

K. Data were corrected for absorption using the empirical method SADABS.[S3] The structures were solved by SHELXT[S4] and refined using the full-matrix least-squares procedures within the SHELXTL software package.[S5] All non-hydrogen atoms were refined with anisotropic displacement parameters. The hydrogen atoms were generated geometrically (C−H = 0.95 Å) using the riding-model.

Data availability. The X-ray crystallographic coordinates for structures reported in this article have been deposited at the Cambridge Crystallographic Data Centre (CCDC), under deposition number CCDC 1849378-1849381 for compounds **Cu_{16}**, **$Cu_{16}\cdot4H_2O$**, **$Cu_{16}\cdot2CH_3OH$** and **$Cu_{16}\cdot2C_2H_5OH$**, respectively. These data can be obtained free of charge from the Cambridge Crystallographic Data Centre via www.ccdc.cam.ac.uk/data_request/cif. All relevant data supporting the findings of this study are available from the corresponding authors on request.

$[Cu^{I}_{16}(L)_8]$ (Cu_{16}). A DMF (8 mL, AR-grade ≥99.7%) solution of $CuSO_4\cdot5H_2O$ (24.9 mg, 0.1 mmol) and H_2L (21.5 mg, 0.075 mmol) was placed in a 15 mL Pyrex vial which was then tightly capped and heated at 140 °C for 48 h. After the autoclave was cooled to 30 °C at a rate of 5 °C h^{-1}, and leave the solution in the Pyrex vial for 3 months, the red square shaped crystals of **Cu_{16}** were collected, washed with DMF, and dried with lens paper (Yield: 4.8 mg, 15% based on the ligand). Elemental analyses (%) calculated for $C_{128}H_{80}N_{48}Cu_{16}$: C, 46.49; H, 2.44; N, 20.33; found: C, 46.61; H, 2.56; N, 20.58. Infrared (KBr, cm^{-1}): 1652(s), 1584(s), 1460(s), 1406(m), 1328(m), 1134(s), 982(w), 764(s), 632(s).

$[Cu^{I}_{16}(L)_8]\cdot4H_2O$ ($Cu_{16}\cdot4H_2O$). The crystals of **Cu_{16}** were soaked in H_2O for 24 h to obtain **$Cu_{16}\cdot4H_2O$**, Elemental analyses (%) calculated for $C_{128}H_{88}N_{48}O_4Cu_{16}$: C, 45.50; H, 2.63; N, 19.90; found: C, 45.88; H, 2.76; N, 19.42. Infrared (KBr, cm^{-1}): 3328(m), 3142(w), 1644(s), 1526(w), 1524(w), 1462(s), 1324(m), 1166(s), 1122(s), 1064(m), 984(w), 766(s), 652(m).

$[Cu^{I}_{16}(L)_8]\cdot2CH_3OH$ ($Cu_{16}\cdot2CH_3OH$). The crystals of **Cu_{16}** were soaked in CH_3OH for 24 h to obtain **$Cu_{16}\cdot2CH_3OH$**, Elemental analyses (%) calculated for $C_{130}H_{88}N_{48}O_2Cu_{16}$: C, 46.32; H, 2.63; N, 19.94; found: C, 46.52; H, 2.44; N, 19.65. Infrared (KBr, cm^{-1}): 3402(m), 3082(w), 1640(s), 1540(w), 1528(w), 1466(s), 1328(m), 1144(s), 1128(s), 1066(m), 990(w), 760(s), 658(m).

$[Cu^{I}_{16}(L)_8]\cdot2C_2H_5OH$ ($Cu_{16}\cdot2C_2H_5OH$). The crystals of **Cu_{16}** were soaked in C_2H_5OH for 24 h to obtain **$Cu_{16}\cdot2C_2H_5OH$**, Elemental analyses (%) calculated for $C_{132}H_{92}N_{48}O_2Cu_{16}$: C, 46.64; H, 2.73; N, 19.78; found: C, 46.44; H, 2.52; N, 19.92. Infrared (KBr, cm^{-1}): 3384(m), 3092(w), 1664(s), 1578(w), 1522(w), 1436(s), 1348(m), 1126(s), 1104(s), 1032(m), 998(w), 748(s), 666(m).

Table S1. Crystallographic data for compounds **Cu_{16}**, **$Cu_{16}\cdot4H_2O$**, **$Cu_{16}\cdot2CH_3OH$** and **$Cu_{16}\cdot2C_2H_5OH$**.

Compound	**Cu_{16}**	**$Cu_{16}\cdot4H_2O$**	**$Cu_{16}\cdot2CH_3OH$**	**$Cu_{16}\cdot2C_2H_5OH$**
Empirical formula	$C_{128}H_{80}N_{48}Cu_{16}$	$C_{128}H_{88}N_{48}O_4Cu_{16}$	$C_{130}H_{88}N_{48}O_2Cu_{16}$	$C_{132}H_{92}N_{48}O_2Cu_{16}$
Formula weight	3307.04	3379.18	3371.20	3399.26
Wavelength (Å)	0.71073	0.71073	0.71073	0.62304
Crystal system	Triclinic	Monoclinic	Monoclinic	Monoclinic
Space group	$P\bar{1}$	$C2/c$	$C2/c$	$C2/c$
a (Å)	15.489(3)	26.031(19)	26.02(2)	25.9893(13)
b (Å)	15.704(3)	16.970(12)	17.081(14)	16.9659(8)
c (Å)	26.649(5)	26.906(19)	27.02(2)	26.8415(13)
α (°)	86.652(4)	90	90	90
β (°)	85.420(5)	91.960(12)	92.033(12)	92.540(2)
γ (°)	68.225(5)	90	90	90
V (Å^3)	5997(2)	11879(15)	12003(17)	11823.6(10)
Z	2	4	4	4
D_c (g cm^{-3})	1.831	1.885	1.861	1.903
T / K	150(2)	150(2)	150(2)	100(2)
F(000)	3296	6720	6704	6752
R_{int}	0.075	0.094	0.168	0.087
R_1[a] [$I \geq 2$ (I)]	0.113	0.101	0.152	0.055
wR_2[b] (all data)	0.280	0.219	0.336	0.148
GoF	1.01	1.07	1.07	1.02

[a] $R_1 = \Sigma||F_o| - |F_c||/\Sigma|F_o|$. [b] $wR_2 = [\Sigma w(F_o^2 - F_c^2)^2/\Sigma w(F_o^2)^2]^{1/2}$

Table S2. Selected bond lengths (Å) and angles (°) for compounds **Cu_{16}**, **$Cu_{16}\cdot 4H_2O$**, **$Cu_{16}\cdot 2CH_3OH$** and **$Cu_{16}\cdot 2C_2H_5OH$**.

		Cu_{16}	
Cu1-N2	1.958(14)	Cu1-N26	2.002(13)
Cu1-N1	2.096(13)	Cu1-N25	2.125(15)
Cu2-N3	1.818(14)	Cu2-N32	1.886(13)
Cu3-N4	1.902(13)	Cu3-N37	2.020(13)
Cu3-N38	2.064(12)	Cu4-N5	2.015(15)
Cu4-N44	2.055(13)	Cu4-N43	2.142(14)
Cu4-N6	2.197(16)	Cu5-N27	1.841(15)
Cu5-N8	1.848(13)	Cu5-N7	2.465(19)
Cu6-N33	1.888(11)	Cu6-N9	1.913(12)
Cu7-N39	1.874(12)	Cu7-N10	1.906(12)
Cu8-N45	1.890(13)	Cu8-N11	2.011(13)
Cu8-N12	2.052(13)	Cu9-N28	1.894(13)
Cu9-N14	1.977(14)	Cu9-N13	2.119(15)
Cu10-N15	1.879(13)	Cu10-N34	1.904(11)
Cu11-N40	1.864(12)	Cu11-N16	1.918(12)
Cu12-N17	1.814(12)	Cu12-N46	1.847(13)
Cu13-N20	1.928(16)	Cu13-N29	1.936(14)
Cu13-N19	2.28(2)	Cu13-N30	2.353(14)
Cu14-N21	1.883(14)	Cu14-N35	2.025(15)
Cu14-N36	2.032(14)	Cu15-N22	1.848(12)
Cu15-N41	1.871(11)	Cu15-N42	2.436(16)
Cu16-N23	1.971(14)	Cu16-N47	2.009(15)
Cu16-N48	2.087(16)	Cu16-N24	2.238(15)
N2-Cu1-N26	123.3(5)	N2-Cu1-N1	79.1(2)
N26-Cu1-N1	126.6(2)	N2-Cu1-N25	138.0(6)
N26-Cu1-N25	78.4(5)	N1-Cu1-N25	118.8(6)
N3-Cu2-N32	173.5(6)	N4-Cu3-N37	152.6(6)
N4-Cu3-N38	119.3(5)	N37-Cu3-N38	81.2(5)
N5-Cu4-N44	153.9(6)	N5-Cu4-N43	113.9(5)
N44-Cu4-N43	78.2(6)	N5-Cu4-N6	80.4(6)
N44-Cu4-N6	110.0(6)	N43-Cu4-N6	130.8(6)

N27-Cu5-N8	169.3(6)	N27-Cu5-N7	113.7(6)
N8-Cu5-N7	75.4(6)	N33-Cu6-N9	159.5(6)
N39-Cu7-N10	171.0(6)	N45-Cu8-N11	120.5(5)
N45-Cu8-N12	151.8(6)	N11-Cu8-N12	80.6(5)
N28-Cu9-N14	128.5(6)	N28-Cu9-N13	143.2(6)
N14-Cu9-N13	80.5(5)	N15-Cu10-N34	167.7(6)
N40-Cu11-N16	158.9(6)	N17-Cu12-N46	174.1(6)
N20-Cu13-N29	171.8(7)	N20-Cu13-N19	76.2(8)
N29-Cu13-N19	108.2(7)	N20-Cu13-N30	110.6(7)
N29-Cu13-N30	126.0(7)	N19-Cu13-N30	126.0(7)
N21-Cu14-N35	121.6(6)	N21-Cu14-N36	147.8(6)
N35-Cu14-N36	81.1(6)	N22-Cu15-N41	169.2(5)
N22-Cu15-N42	114.1(5)	N41-Cu15-N42	75.6(5)
N23-Cu16-N47	122.9(5)	N23-Cu16-N48	134.7(6)
N47-Cu16-N48	79.7(6)	N23-Cu16-N24	77.5(6)
N47-Cu16-N24	140.8(6)	N48-Cu16-N24	110.7(6)
		Cu_{16}·$4H_2O$	
Cu1-N14	1.973(11)	Cu1-N2	1.995(11)
Cu1-N1	2.105(12)	Cu1-N13	2.115(11)
Cu2-N8	1.833(11)	Cu2-N15	1.835(11)
Cu3-N16	1.880(11)	Cu3-N24^{i}	1.988(11)
Cu3-N23^{i}	2.022(10)	Cu4-N17^{i}	1.987(10)
Cu4-N17	1.987(10)	Cu4-N18	2.039(12)
Cu4-N18^{i}	2.039(12)	Cu5-N3	1.838(11)
Cu5-N20	1.842(11)	Cu5-N19	2.339(12)
Cu6-N21	1.886(11)	Cu6-N9	1.900(11)
Cu7-N22^{i}	1.848(10)	Cu7-N22	1.848(10)
Cu8-N4	1.878(11)	Cu8-N12^{i}	2.017(11)
Cu8-N11^{i}	2.024(11)	Cu9-N10^{i}	1.879(10)
Cu9-N10	1.879(10)	Cu10-N5^{i}	1.950(11)
Cu10-N5	1.950(11)	Cu10-N6^{i}	2.002(12)
Cu10-N6	2.002(12)	N14-Cu1-N2	119.2(4)
N14-Cu1-N1	141.5(5)	N2-Cu1-N1	79.0(4)
N14-Cu1-N13	79.4(4)	N2-Cu1-N13	125.2(4)
N1-Cu1-N13	119.5(5)	N8-Cu2-N15	174.3(5)

N16-Cu3-N24^{i}	153.1(5)	N16-Cu3-N23^{i}	116.7(4)
N24^{i}-Cu3-N23^{i}	82.1(4)	N17^{i}-Cu4-N17	161.7(7)
N17^{i}-Cu4-N18	106.4(4)	N17-Cu4-N18	80.3(4)
N17^{i}-Cu4-N18^{i}	80.3(4)	N17-Cu4-N18^{i}	106.6(4)
N18-Cu4-N18^{i}	136.6(7)	N17^{i}-Cu4-N7^{i}	80.9(3)
N17-Cu4-N7^{i}	80.9(3)	N18-Cu4-N7^{i}	111.7(3)
N18^{i}-Cu4-N7^{i}	111.7(3)	N3-Cu5-N20	167.0(5)
N3-Cu5-N19	116.3(5)	N20-Cu5-N19	76.7(4)
N21-Cu6-N9	161.1(4)	N22^{i}-Cu7-N22	168.1(7)
N22^{i}-Cu7-N6^{i}	98.7(3)	N22-Cu7-N6^{i}	88.2(3)
N4-Cu8-N12^{i}	146.8(5)	N4-Cu8-N11^{i}	117.5(4)
N12^{i}-Cu8-N11^{i}	82.2(4)	N10^{i}-Cu9-N10	166.2(7)
N10^{i}-Cu9-N6^{i}	95.5(3)	N10-Cu9-N6^{i}	92.5(3)
N5^{i}-Cu10-N5	169.3(7)	N5^{i}-Cu10-N6^{i}	81.6(4)
N5-Cu10-N6^{i}	102.8(4)	N5^{i}-Cu10-N6	102.8(4)
N5-Cu10-N6	81.6(4)	N6^{i}-Cu10-N6	132.2(7)
		Cu_{16}·2CH_3OH	
Cu1-N14	1.979(18)	Cu1-N2	1.980(18)
Cu1-N1	2.09(2)	Cu1-N13	2.111(17)
Cu2-N3	1.839(18)	Cu2-N20	1.869(18)
Cu2-N19	2.31(2)	Cu3-N4	1.885(16)
Cu3-N12^{i}	2.017(17)	Cu3-N11^{i}	2.069(17)
Cu4-N5^{i}	1.977(18)	Cu4-N5	1.977(17)
Cu4-N6^{i}	2.017(19)	Cu4-N6	2.017(19)
Cu5-N15	1.835(19)	Cu5-N8	1.867(17)
Cu6-N21	1.905(17)	Cu6-N9	1.910(16)
Cu7-N10	1.889(17)	Cu7-N10^{i}	1.889(17)
Cu8-N16	1.888(16)	Cu8-N23^{i}	2.011(18)
Cu8-N24^{i}	2.016(17)	Cu9-N22^{i}	1.873(15)
Cu9-N22	1.873(15)	Cu10-N17	1.998(18)
Cu10-N17^{i}	1.998(18)	Cu10-N18^{i}	2.072(19)
Cu10-N18	2.072(19)		
N14-Cu1-N2	119.2(7)	N14-Cu1-N1	143.1(8)
N2-Cu1-N1	78.6(8)	N14-Cu1-N13	78.8(7)
N2-Cu1-N13	125.1(8)	N1-Cu1-N13	119.3(7)

N3-Cu2-N20	166.6(7)	N3-Cu2-N19	116.4(8)
N20-Cu2-N19	76.9(7)	N4-Cu3-N12^{i}	148.6(8)
N4-Cu3-N11^{i}	118.5(7)	N12^{i}-Cu3-N11^{i}	80.8(7)
N5^{i}-Cu4-N5	167.8(11)	N5^{i}-Cu4-N6^{i}	81.1(8)
N5-Cu4-N6^{i}	104.1(8)	N5^{i}-Cu4-N6	104.1(8)
N5-Cu4-N6	81.1(8)	N6^{i}-Cu4-N6	130.5(11)
N15-Cu5-N8	174.6(8)	N21-Cu6-N9	159.5(8)
N10-Cu7-N10^{i}	164.6(11)	N10-Cu7-Cu6^{i}	92.7(5)
N10^{i}-Cu7-Cu6^{i}	96.2(5)	N16-Cu8-N23^{i}	118.6(7)
N16-Cu8-N24^{i}	152.5(8)	N23^{i}-Cu8-N24^{i}	82.0(8)
N22^{i}-Cu9-N22	169.3(12)	N22^{i}-Cu9-Cu6^{i}	99.2 (6)
N22-Cu9-Cu6^{i}	87.2(6)	N17-Cu10-N17^{i}	157.7(10)
N17-Cu10-N18^{i}	107.6(7)	N17^{i}-Cu10-N18^{i}	81.1(7)
N17Cu10N18	81.1(7)	N17^{i}-Cu10-N18	107.6(7)
N18^{i}-Cu10-N18	135.3(12)		

Cu_{16}·$2C_2H_5OH$

Cu1-N2	1.988(5)	Cu1-N14	1.995(5)
Cu1-N1	2.080(5)	Cu1-N13	2.113(5)
Cu2-N3	1.853(5)	Cu2-N20	1.859(4)
Cu2-N19	2.324(5)	Cu3-N4	1.888(4)
Cu3-N12^{i}	1.995(5)	Cu3-N11^{i}	2.036(4)
Cu4-N5	1.962(4)	Cu4-N5^{i}	1.962(4)
Cu4-N6^{i}	2.005(5)	Cu4-N6	2.005(5)
Cu5-N15	1.842(4)	Cu5-N8	1.850(4)
Cu6-N9	1.889(4)	Cu6-N21	1.891(4)
Cu7-N10^{i}	1.883(4)	Cu7-N10	1.883(4)
Cu8-N16	1.898(4)	Cu8-N24^{i}	2.009(5)
Cu8-N23^{i}	2.037(4)	Cu9-N22	1.872(4)
Cu9-N22^{i}	1.872(4)	Cu10-N17	1.983(4)
Cu10-N17^{i}	1.983(4)	Cu10-N18^{i}	2.091(5)
Cu10-N18	2.091(5)	N2-Cu1-N14	118.64(17)
N2-Cu1-N1	79.66(18)	N14-Cu1-N1	141.6(2)
N2-Cu1-N13	124.13(19)	N14-Cu1-N13	79.01(18)
N1-Cu1-N13	120.46(19)	N3-Cu2-N20	166.61(19)
N3-Cu2-N19	116.48(17)	N20-Cu2-N19	76.87(17)

N4-Cu3-N12^{i}	148.0(2)	N4-Cu3-N11^{i}	116.54(17)
N12^{i}-Cu3-N11^{i}	82.34(7)	N5-Cu4-N5^{i}	167.5(3)
N5-Cu4-N6^{i}	103.76(18)	N5^{i}-Cu4-N6^{i}	81.26(18)
N5-Cu4-N6	81.26(18)	N5^{i}-Cu4-N6	103.77(18)
N6^{i}-Cu4-N6	133.5(3)	N15-Cu5-N8	174.3(2)
N9-Cu6-N21	161.05(17)	N9-Cu6-N7^{i}	92.41(13)
N21-Cu6-N7^{i}	102.18(13)	N10^{i}-Cu7-N10	165.4(3)
N16-Cu8-N24^{i}	153.5(2)	N16-Cu8-N23^{i}	117.40(17)
N24^{i}-Cu8-N23^{i}	81.67(17)	N22-Cu9-N22^{i}	169.3(3)
N22-Cu9-N6^{i}	87.87(13)	N22^{i}-Cu9-N6^{i}	98.38(12)
N17-Cu10-N17^{i}	159.9(3)	N17-Cu10-N18^{i}	108.24(18)
N17^{i}-Cu10-N18^{i}	79.67(18)	N17-Cu10-N18	79.67(18)
N17^{i}-Cu10-N18	108.24(18)	N18^{i}-Cu10-N18	135.0(3)

Symmetry code for **Cu_{16}·4H_2O**: (i) -*x*+1, *y*, -*z*+1/2; for **Cu_{16}·2CH_3OH**: (i) -*x*+1, *y*, -*z*+3/2; for **Cu_{16}·2C_2H_5OH**: (i) -*x*+1, *y*, -*z*+3/2.

Table S3. Copper-copper bond lengths (Å) for compounds **Cu_{16}**, **Cu_{16}·4H_2O**, **Cu_{16}·2CH_3OH** and **Cu_{16}·2C_2H_5OH**.

Atom-Atom	**Cu_{16}**	**Cu_{16}·4H_2O**	**Cu_{16}·2CH_3OH**	**Cu_{16}·2C_2H_5OH**
Cu1-Cu2	3.4818 3.4334	3.4317	3.4042	3.4085
Cu1-Cu5	3.3872 3.3397	3.3932	3.4527	3.4503
Cu2-Cu3	2.6034 2.6014	2.5727	2.5653	2.5614
Cu2-Cu5	3.3299 3.2821	3.2236	3.2284	3.2309
Cu2-Cu6	2.8781 2.8491	2.8415	3.0431	3.0426
Cu3-Cu4	3.6415 3.6343	3.6591	3.6322	3.6509
Cu3-Cu6	3.6063 3.5134	3.5515	3.6263	3.6236
Cu3-Cu7	3.6231 3.6180	3.7076	3.7269	3.7431
Cu4-Cu7	3.1486	3.0432	2.9704	2.9680
Cu5-Cu6	3.0223 3.0025	3.0279	2.8482	2.8382
Cu5-Cu8	2.5980 2.6108	2.5650	2.5882	2.5790

Cu6-Cu7	2.7230 2.7032	2.7051	2.6993	2.6932
Cu6-Cu8	3.7044 3.5574	3.6153	3.5491	3.5497
Cu6-Cu9	2.7027 2.6860	2.6922	2.7141	2.7084
Cu7-Cu9	3.2408	3.1274	3.1566	3.1397
Cu8-Cu9	3.6040 3.4939	3.7248	3.6932	3.6881
Cu8-Cu10	3.4574 3.3370	3.6302	3.6689	3.6502
Cu9-Cu10	2.9825	2.9647	3.0695	3.0610

Table S4. Hydrogen-bond geometry (Å, º) for **Cu_{16}·4H_2O**. (D, donor atom; A, acceptor atom).

D-H···*A*	*D*···*A*	*D*-H···*A*
C2-H2···O2a^{ii}	3.34 (3)	145
C13-H13···O2a	3.20 (3)	165
C15-H15···N13^{iii}	3.27 (2)	120
C29-H29···O1′b^{iv}	3.28 (3)	133
C47-H47···O1′b^{v}	3.36 (3)	168

Symmetry code: (ii) -*x*+3/2, -*y*+3/2, -*z*+1; (iii) *x*-1/2, *y*+1/2, *z*; (iv) -*x*+1, -*y*+2, -*z*+1; (v) -*x*+1, *y*-1, -*z*+1/2.

Table S5. Hydrogen-bond geometry (Å, º) for **Cu_{16}·2CH_3OH**. (D, donor atom; A, acceptor atom).

D-H···*A*	D···*A*	D-H···*A*
C13-H13···O1′^{b}	3.15 (5)	154
C29-H29···O1a^{ii}	3.30 (6)	128
C47-H47···O1a^{iii}	3.51 (6)	160

Symmetry code: (ii) -*x*+1, -*y*, -*z*+1; (iii) -*x*+1, *y*+1, -*z*+3/2.

Table S6. Hydrogen-bond geometry (Å, º) for **Cu_{16}·2C_2H_5OH**. (D, donor atom; A, acceptor atom).

D-H···*A*	*D*···*A*	*D*-H···*A*
C2-H2···O1′a^{ii}	3.195 (14)	141
C13-H13···O1′a	3.185 (13)	164
C29-H29···O1b^{iii}	3.245 (13)	131
C47-H47···O1b^{iv}	3.269 (13)	169

Symmetry code: (ii) -*x*+1/2, -*y*+1/2, -*z*+1; (iii) -*x*+1, -*y*, -*z*+1; (iv) -*x*+1, *y*+1, -*z*+3/2.

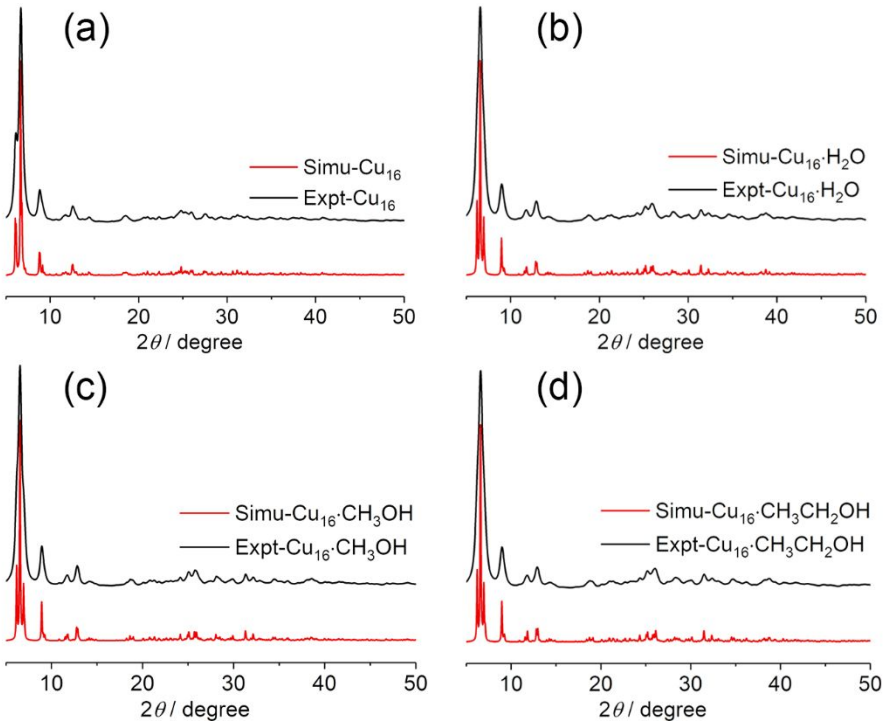

Figure S1. Experimental (Expt.) and simulated (Simu.) PXRD patterns of (a) **Cu_{16}**, (b) **$Cu_{16}·4H_2O$**, (c) **$Cu_{16}·2CH_3OH$** and (d) **$Cu_{16}·2C_2H_5OH$**.

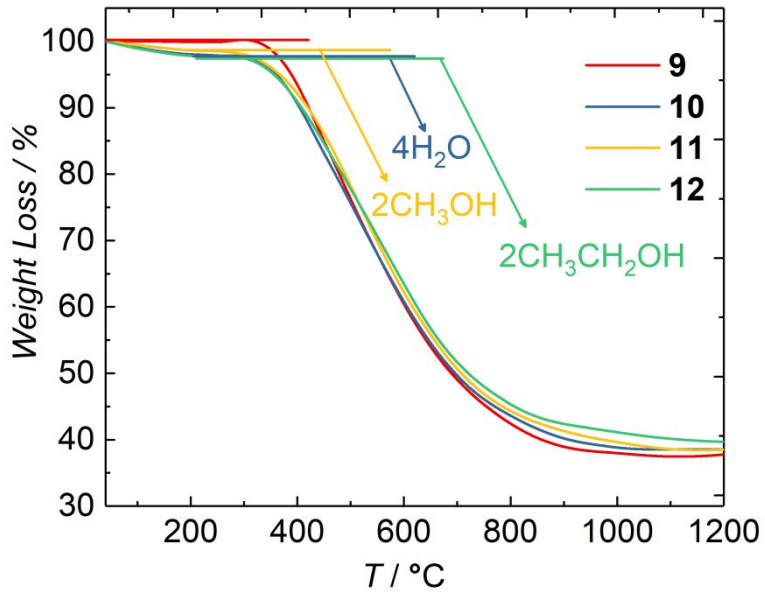

Figure S2. Thermogravimetric analyses of **Cu_{16}**, **$Cu_{16}·4H_2O$**, **$Cu_{16}·2CH_3OH$** and **$Cu_{16}·2C_2H_5OH$** under N_2. The heating rate was 5 °C min^{-1} from 40 to 1200 °C.

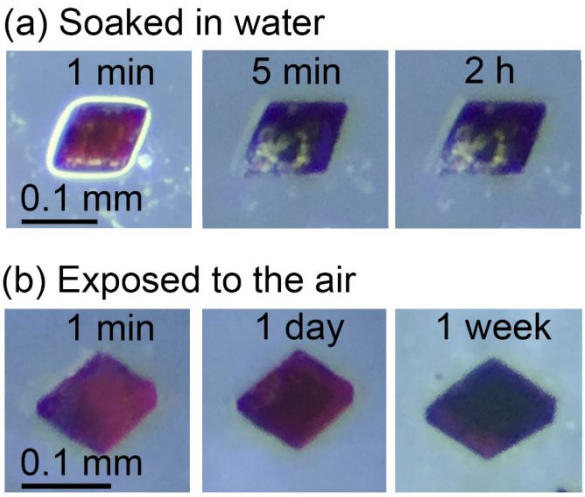

Figure S3. Views of the single crystal of **Cu_{16}** were (a) soaked in water and (b) exposed to the air.

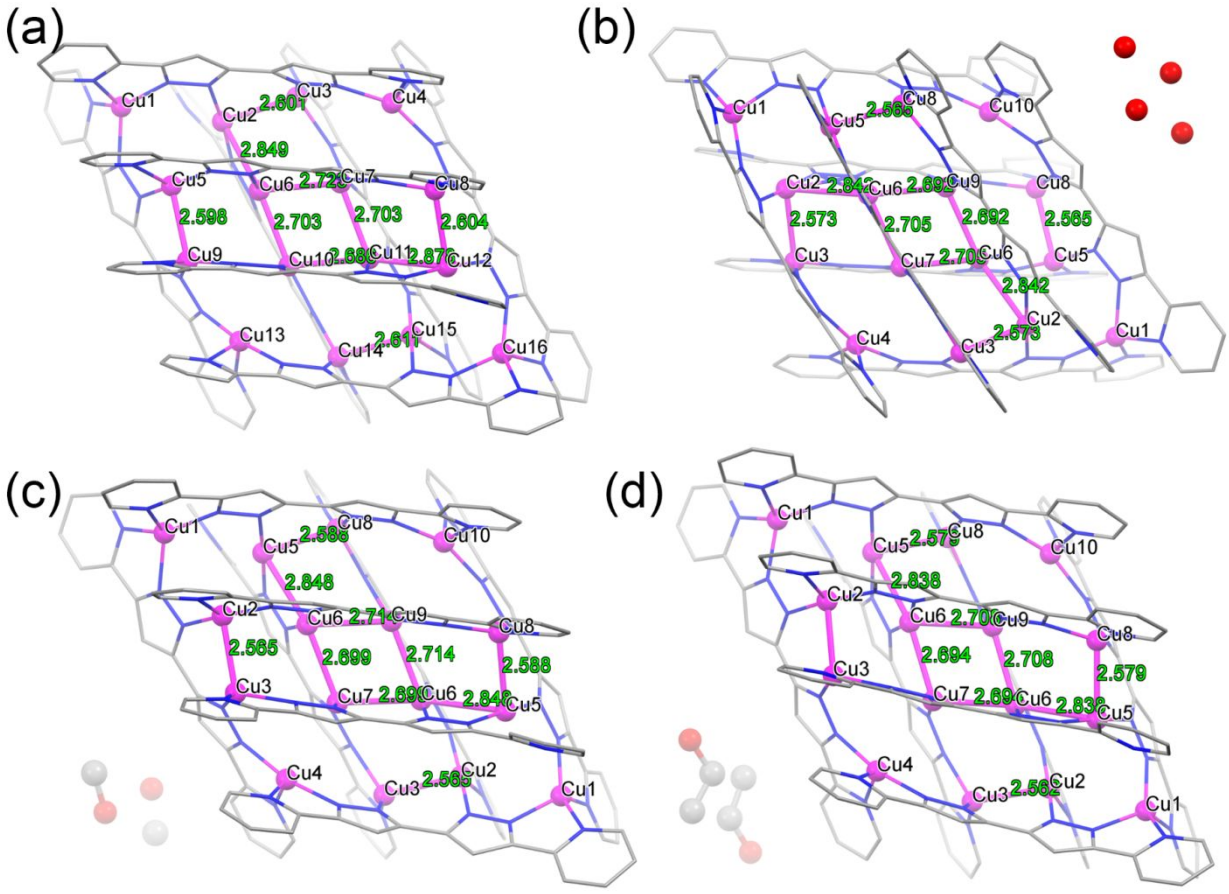

Figure S4. Views of the crystal structures of (a) **Cu_{16}**, (b) **$Cu_{16}·4H_2O$**, (c) **$Cu_{16}·2CH_3OH$** and (d) **$Cu_{16}·2C_2H_5OH$**.

Table S7. Range of the metrics observed for 5,5′-pyridyl-3,3′-bis-1*H*-pyrazolate.

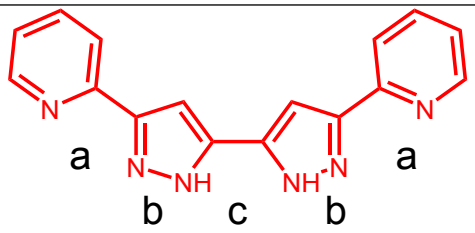

Distance (Å)	a	b	c
Minimum	2.50	1.30	2.44
Maximum	2.95	1.41	3.02

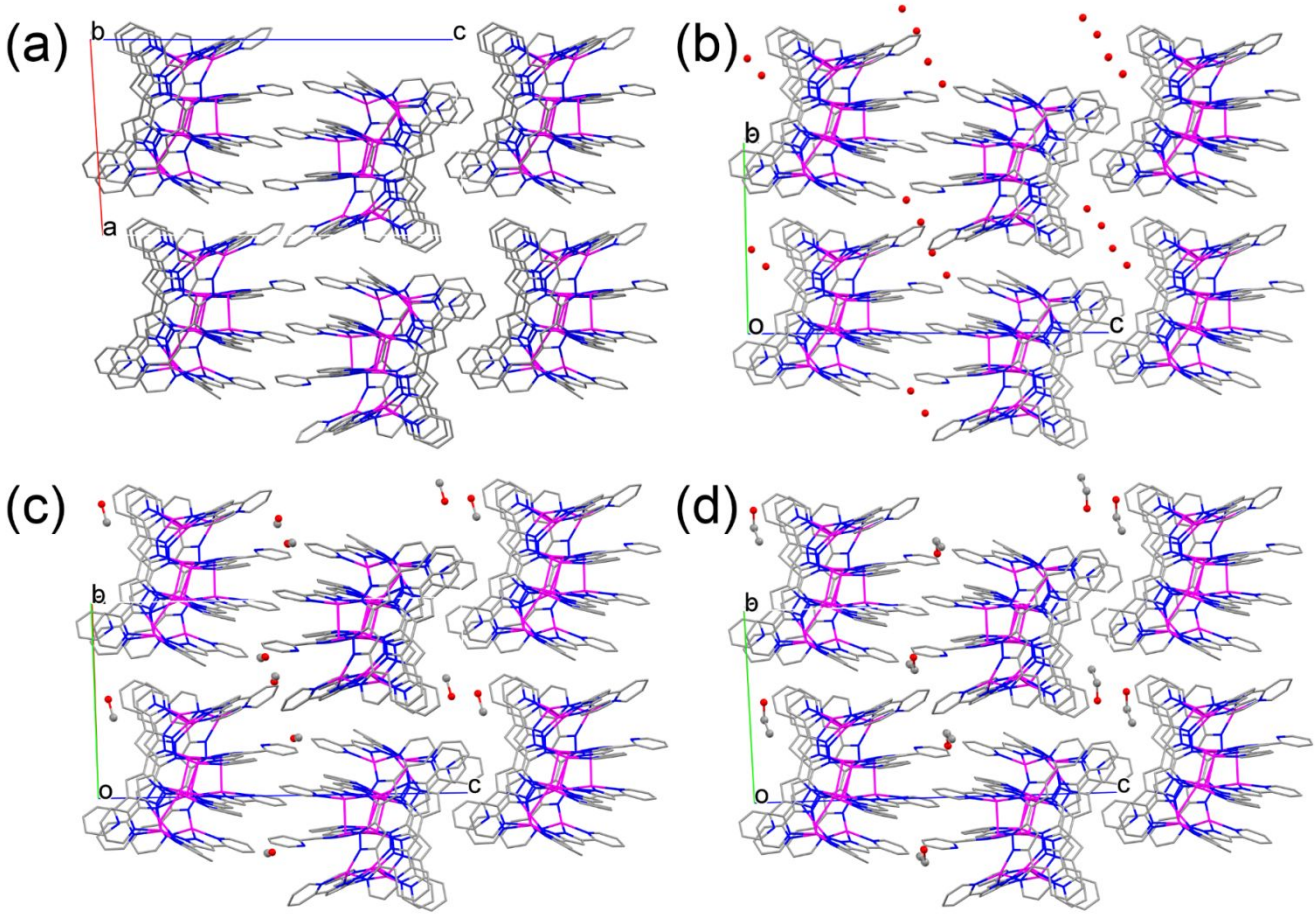

Figure S5. Views of the crystal packing of (a) **Cu_{16}**, (b) **Cu_{16}·$4H_2O$**, (c) **Cu_{16}·$2CH_3OH$** and (d) **Cu_{16}·$2C_2H_5OH$**.

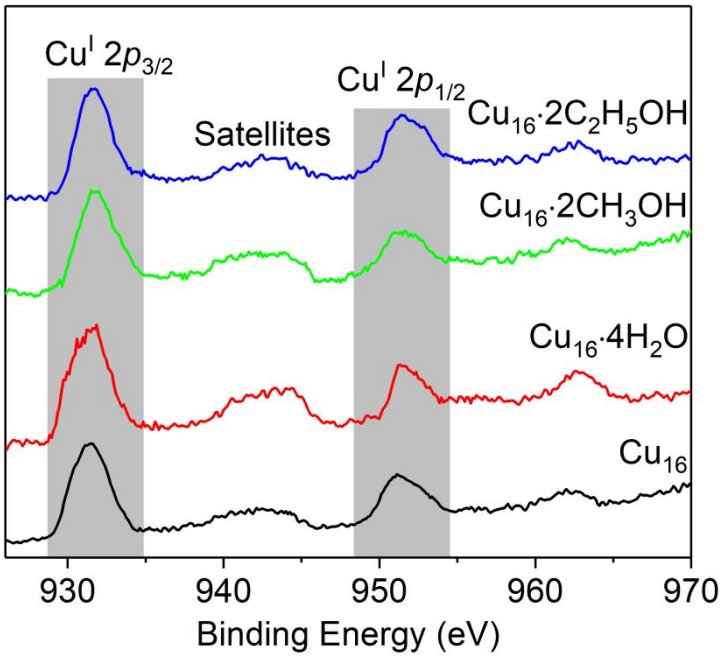

Figure S6. Cu-2$p_{3/2}$ and Cu-2$p_{1/2}$ valence band XPS spectra for **Cu$_{16}$**, **Cu$_{16}$·4H$_2$O**, **Cu$_{16}$·2CH$_3$OH** and **Cu$_{16}$·2C$_2$H$_5$OH**.

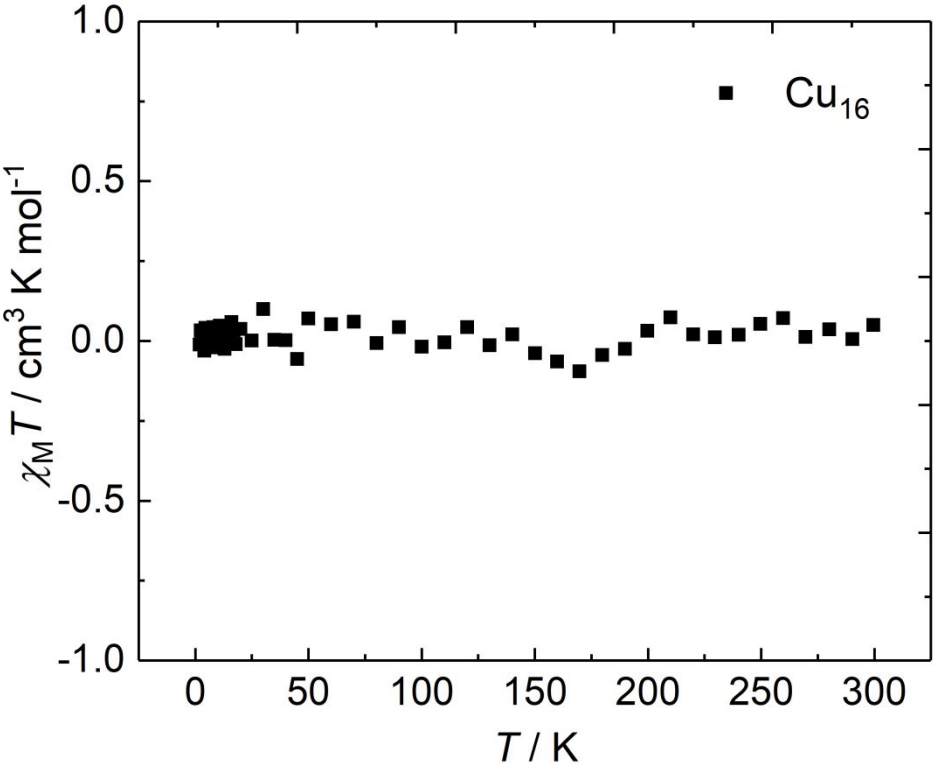

Figure S7. Temperature dependence of $\chi_M T$ for **Cu$_{16}$** measured in a field of 1.0 kOe.

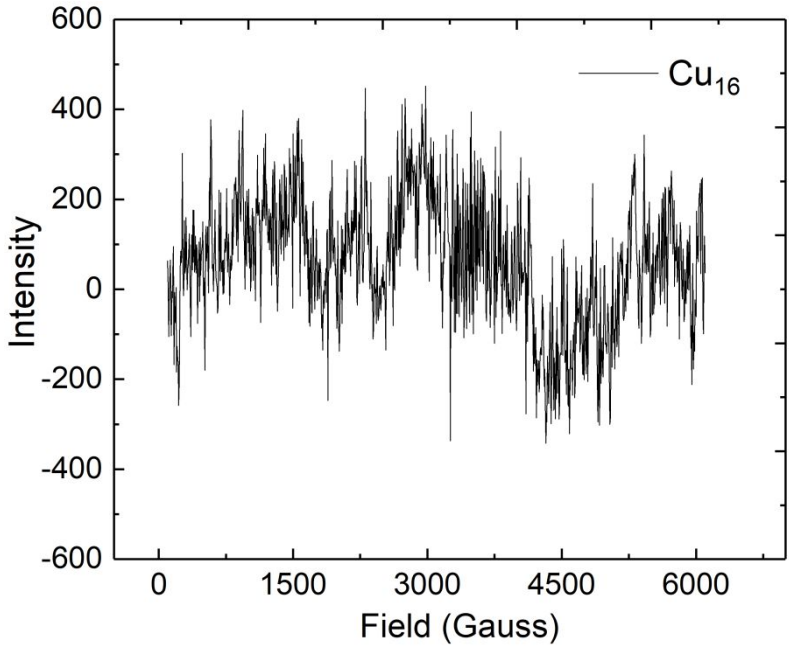

Figure S8. X-band EPR spectrum of a randomly oriented polycrystalline sample of **Cu_{16}** at 298 K, at a microwave frequency of 9.545 GHz and power of 0.189 mW.

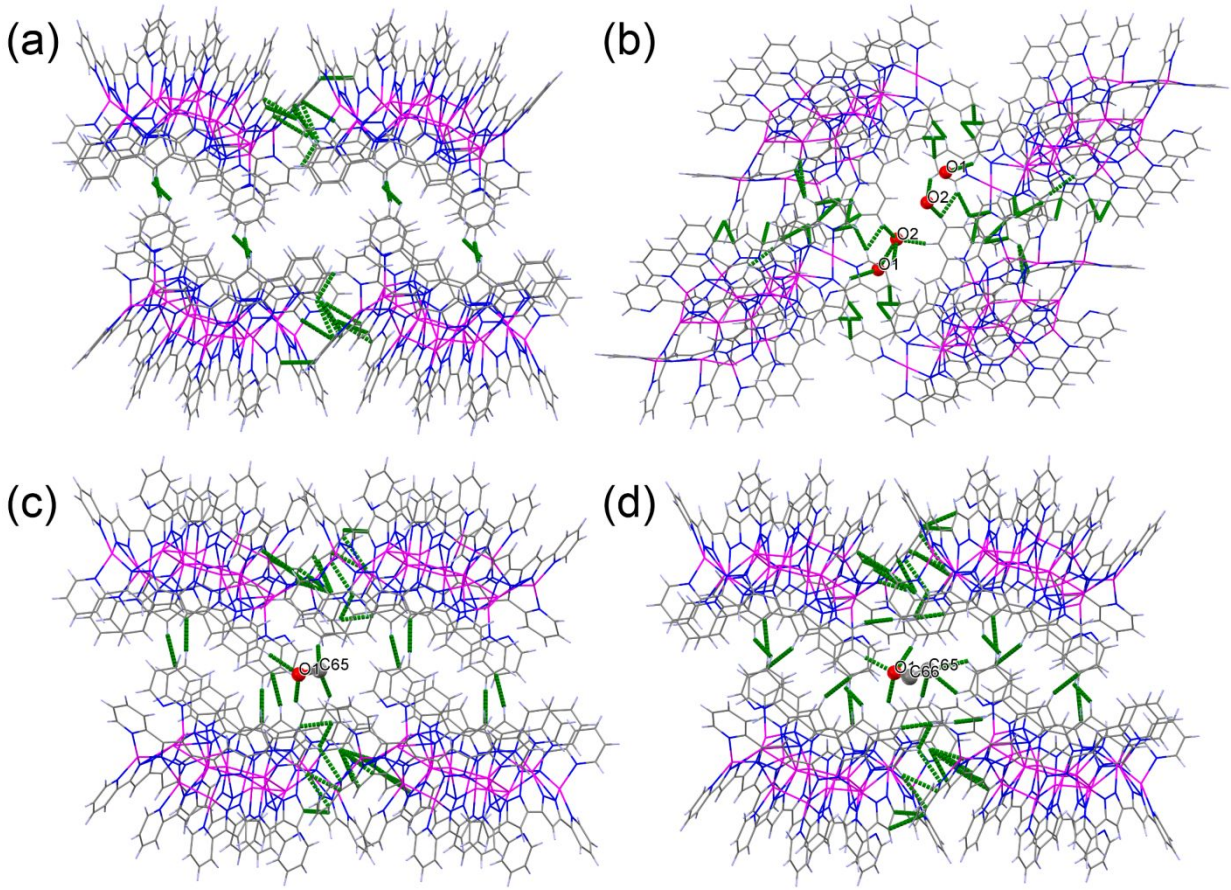

Figure S9. Weak supramolecular interactions between the solvent molecules and the host frameworks of (a) **Cu_{16}**, (b) **$Cu_{16}\cdot 4H_2O$**, (c) **$Cu_{16}\cdot 2CH_3OH$** and (d) **$Cu_{16}\cdot 2C_2H_5OH$**.

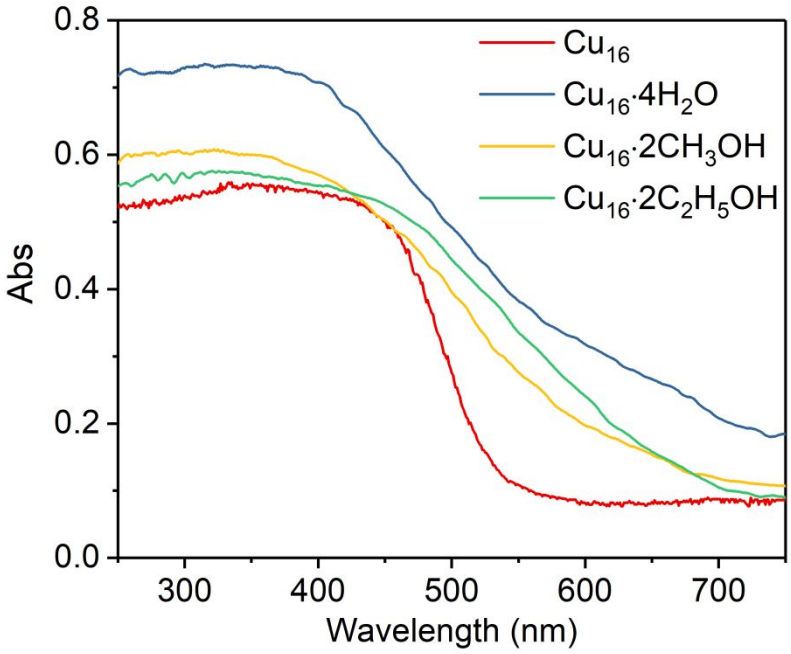

Figure S10. Solid-state UV-vis spectra of **Cu_{16}**, **$Cu_{16}·4H_2O$**, **$Cu_{16}·2CH_3OH$** and **$Cu_{16}·2C_2H_5OH$**. The darkening of the crystals is associated with the broadening of the sharp edge of **Cu_{16}** centered at ca. 480 nm.

References

S1. Yu, F.; Li, J.; Cao, Z.-H.; Kurmoo, M.; Zuo, J.-L. Electrical Conductivity of Copper Hexamers Tuned by their Ground-State Valences. *Inorg. Chem.* **2018**, *57*, 3443−3450.

S2. *Mercury CSD 3.9 (Build RC1)*, CCDC, 2016.

S3. Sheldrick, G. M. *SADABS—Bruker AXS Area Detector Scaling and Absorption;* 2008.

S4. Sheldrick, G. M. SHELXT-Integrated Space-group and Crystal-structure Determination. *Acta Crystallogr., Sect. A:* **2015**, *A71*, 3–8.

S5. Sheldrick, G. M. Crystal structure refinement with SHELXL. *Acta Crystallogr., Sect. C.* **2015***, C71,* 3–8.